Cell, Vol. 120, 649–661, March 11, 2005, Copyright ©2005 by Elsevier Inc. DOI 10.1016/j.cell.2004.12.041

Reactive Oxygen Species Promote TNFα-Induced Death and Sustained JNK Activation by Inhibiting MAP Kinase Phosphatases

Hideaki Kamata,[1,2,3] Shi-ichi Honda,[3] Shin Maeda,[1,2] Lufen Chang,[1,2] Hajime Hirata,[3] and Michael Karin[1,2,*]
[1]Laboratory of Gene Regulation and Signal Transduction
[2]Department of Pharmacology
School of Medicine
University of California, San Diego
9500 Gilman Drive
La Jolla, California 92093
[3]Graduate School of Life Science
University of Hyogo
Khoto 3-2-1, Kamigori
Hyogo, 678-1297
Japan

Summary

TNFα is a pleiotropic cytokine that induces either cell proliferation or cell death. Inhibition of NF-κB activation increases susceptibility to TNFα-induced death, concurrent with sustained JNK activation, an important contributor to the death response. Sustained JNK activation in NF-κB-deficient cells was suggested to depend on reactive oxygen species (ROS), but how ROS affect JNK activation was unclear. We now show that TNFα-induced ROS, whose accumulation is suppressed by mitochondrial superoxide dismutase, cause oxidation and inhibition of JNK-inactivating phosphatases by converting their catalytic cysteine to sulfenic acid. This results in sustained JNK activation, which is required for cytochrome c release and caspase 3 cleavage, as well as necrotic cell death. Treatment of cells or experimental animals with an antioxidant prevents H_2O_2 accumulation, JNK phosphatase oxidation, sustained JNK activity, and both forms of cell death. Antioxidant treatment also prevents TNFα-mediated fulminant liver failure without affecting liver regeneration.

Introduction

Tumor necrosis factor (TNF)α is a pleiotropic cytokine that triggers either cell proliferation, cell death, or inflammation through two distinct receptors: TNF receptor (TNFR) 1 and 2 (Wajant et al., 2003). These responses depend on effector pathways, including mitogen-activated protein kinases (MAPKs) that activate AP-1 transcription factors and IκB kinases (IKK) that activate NF-κB (Brenner et al., 1989; DiDonato et al., 1997; Liu et al., 1996).

NF-κB is a major negative regulator of programmed cell death (PCD), especially in response to TNFα and similar cytokines (Karin and Lin, 2002). If NF-κB activation is prevented, TNFα can induce either apoptotic or necrotic cell death (Fiers et al., 1999). Several mechanisms account for this activity of NF-κB, including induction of antiapoptotic members of the Bcl2 family and caspase inhibitors (Karin and Lin, 2002). Another less understood mechanism entails inhibition of sustained Jun N-terminal kinase (JNK) activation (De Smaele et al., 2001; Sakon et al., 2003; Tang et al., 2001). Initially, JNK activation was found not to be required for PCD in certain types of cells treated with TNFα plus inhibitors of RNA or protein synthesis (Liu et al., 1996). However, the use of such inhibitors can result in artifactual results (Deng et al., 2003), and it is generally agreed that in cells lacking the major activating subunit of NF-κB, RelA(p65), the IKKβ subunit of the IKK complex or upstream components of the TNFR1 signaling machinery, JNK activation is an important mediator of PCD. Certain cytokines, drugs, or viruses may also interfere with NF-κB activation and thereby cause sustained JNK activation and enhance TNFα-induced PCD in genetically normal subjects.

In NF-κB-competent cells, TNFα leads to rapid but transient JNK activation that after peaking within 15–30 min is terminated within 60 min (Liu et al., 1996), due to the action of JNK phosphatases (Cavigelli et al., 1996). This response is dramatically extended in NF-κB-deficient cells (De Smaele et al., 2001; Tang et al., 2001) or mice (Maeda et al., 2003). Whereas administration of lipopolysaccharide (LPS) to mice lacking IKKβ in liver cells (*Ikkβ*$^{\Delta hep}$ mice) results in transient JNK activation and little liver injury, administration of concanavalin A (ConA), a pan-T cell activator, causes sustained JNK activation, massive liver cell death (both apoptosis and necrosis), and liver failure (Maeda et al., 2003). Similar hepatotoxicity is observed in wild-type (wt) mice exposed to higher concentrations of ConA or a combination of ConA and N-acetyl-galactosamine, a toxic compound that blocks transcription in hepatocytes. ConA-induced hepatitis is a reasonable model for fulminant liver failure in humans, and it is likely that other hepatotoxins or viruses that cause acute liver failure may do so through inhibition of NF-κB. JNK-deficient mice are relatively immune to these toxic challenges, exhibiting considerably less liver apoptosis and necrosis (Maeda et al., 2003). Unlike ConA challenge, partial hepatectomy, which also induces TNFα expression, causes transient JNK activation that like its upstream activator, TNFR1 (Yamada et al., 1997), is instrumental in liver regeneration (Schwabe et al., 2003). For therapeutic purposes, it is desirable to convert the TNFα-mediated death response to a regenerative response. We thus wished to further understand how reduced NF-κB activity leads to sustained JNK activation and consequently more PCD in ConA-challenged mice.

Several mechanisms were proposed to explain the crosstalk between NF-κB and JNK, including induction of GADD45β (De Smaele et al., 2001) and XIAP (Tang et al., 2001). However, analysis of *Gadd45β*$^{-/-}$ or *Xiap*$^{-/-}$ fibroblasts failed to reveal changes in the kinetics of JNK activation (Amanullah et al., 2003; Kucharczak et al., 2003). More recently, it was suggested that reactive oxygen species (ROS), whose production is induced by TNFα, are responsible for sustained JNK activation (Sa-

*Correspondence: karinoffice@ucsd.edu

kon et al., 2003). Whereas XIAP and GADD45β inhibit PCD (Deveraux et al., 1997; Smith et al., 1996), ROS production causes cell death (Fiers et al., 1999). Curiously, NF-κB activates the SOD2 gene, which encodes a mitochondrial form of the antioxidant enzyme superoxide dismutase (SOD) that inhibits TNFα-induced PCD (Wong et al., 1989). TNFα-induced PCD can also be suppressed by chemical antioxidants, such as butylated hydroxyanisole (BHA) (Goossens et al., 1995; Sakon et al., 2003; Vercammen et al., 1998). Although such results underscore a role for ROS in PCD, a defined target for ROS-mediated oxidation that promotes TNFα-induced death was lacking (Cai and Jones, 1998; Fiers et al., 1999).

We undertook a detailed investigation of the proposed involvement of ROS in the crosstalk between NF-κB and JNK and TNFα-induced PCD. We confirmed that exposure of NF-κB-deficient cells to TNFα, but not IL-1, results in massive but delayed H_2O_2 accumulation. Increased oxidative stress is also seen in ConA-challenged *Ikkβ*$^{\Delta hep}$ mice. Importantly, intracellular H_2O_2 accumulation inactivates MAPK phosphatases (MKPs), by oxidation of their catalytic cysteine. This leads to sustained activation of JNK and p38 MAPK. Expression of catalytically inactive MKPs prolongs JNK activation and potentiates TNFα-induced killing of NF-κB-competent cells. TNFα-induced PCD is also potentiated by inhibition of thioredoxin (Trx)-reductase (TrxR), an enzyme whose activity is required for recycling of oxidized MKPs. Inhibition of ROS accumulation preserves MKP activity, blocks sustained JNK activation, and prevents ConA-induced liver destruction, but has no effect on liver regeneration after partial hepatectomy.

Results

TNFα-Induced ROS Cause Sustained JNK Activation and Cell Death

We examined JNK and p38 activation in mouse fibroblasts that are either wt or deficient for either IKKβ or RelA(p65). As expected, JNK and p38 were transiently activated by either TNFα or IL-1 in wt fibroblasts. TNFα, but not IL-1, led to sustained JNK and p38 activation in both RelA- and IKKβ-deficient fibroblasts (Figure S1A). As shown previously (Sakon et al., 2003), BHA suppressed the sustained phase of JNK and p38 activation in RelA- and IKKβ-deficient fibroblasts, restoring transient kinase activation (Figure S1A). As TNFα is a poor activator of ERK in fibroblasts, we were not able to examine whether BHA or NF-κB deficiency affect ERK activity.

Sensitivity to BHA suggested the involvement of ROS in sustained MAPK activation. Indeed, flow cytometric analysis of cells incubated with the H_2O_2-sensitive fluorescent dye, CM-H_2DCFDA, confirmed substantial accumulation of H_2O_2 in RelA- and IKKβ-deficient fibroblasts after TNFα treatment but not after incubation with IL-1 (Figure S1B and data not shown). The kinetics of ROS accumulation were slow and paralleled those of TNFα-induced PCD (Figure 1A). BHA suppressed TNFα-induced ROS accumulation (Figures 1A and S1B) and conferred resistance to PCD (Figure 1A). TNFα can induce either apoptotic or necrotic cell death (Fiers et al., 1999), and BHA was shown to mainly suppress TNFα-induced necrosis (Sakon et al., 2003). To examine the type of PCD induced by TNFα in *Ikkβ*$^{-/-}$ cells, we measured permeability to propidium iodide (PI) to monitor loss of membrane integrity—a general marker of cell death and changes in cell volume. Apoptosis reduces cell volume, whereas necrosis does not (Vanden Berghe et al., 2004). Flow cytometric analysis revealed that TNFα induced both apoptosis and necrosis of *Ikkβ*$^{-/-}$ fibroblasts and that BHA suppressed both types of death (Figure 1B). Both forms of death were induced concomitantly (Figures S2 and S3).

Consistent with a role for ROS in TNFα-induced apoptosis, the kinetics of H_2O_2 production were similar to those of cytochrome c release and cleavage of caspase 3, both of which were prevented by BHA (Figure 1C). Cytochrome c release and caspase 3 cleavage are also seen upon ConA administration to mice. Both TNFα- and ConA-induced cytochrome c release and caspase 3 cleavage were blocked by deletion of JNK1 (Figure 1D and data not shown).

MnSOD Suppresses TNFα-Induced ROS Production and Cell Death

MnSOD is an important NF-κB-dependent antioxidant that can protect cells from TNFα-induced PCD (Wong et al., 1989). We confirmed that TNFα markedly induced MnSOD in wt but not *Ikkβ*$^{-/-}$ fibroblasts (Figure 1E). To examine whether MnSOD deficiency contributes to ROS accumulation, we stably transfected *Ikkβ*$^{-/-}$ fibroblasts with an MnSOD expression vector and established pooled *Ikkβ*$^{-/-}$ (MnSOD) cells, in which ectopic MnSOD was constitutively expressed, but only at 30%–40% of the amount seen in TNFα-treated wt fibroblasts (Figure 1E). Nonetheless, this was sufficient to significantly inhibit TNFα-induced H_2O_2 accumulation and PCD (Figures 1F and 1G). Thus, the mitochondrion, the site of MnSOD expression, is an important source of ROS in TNFα-stimulated *Ikkβ*$^{-/-}$ cells.

Inhibition of JNK Phosphatases in TNFα-Treated Cells

All MAPKs are activated through tyrosine and threonine phosphorylation at their activation loops by MAPK kinases (MKKs) and are inactivated by dephosphorylation of the same sites by MKPs (Davis, 2000). Sustained JNK activation could therefore involve either an upstream kinase or inhibition of JNK phosphatases. A MKK kinase (MAP3K) responsive to both TNFα and H_2O_2 is ASK1 (Takeda et al., 2003). However, no ASK1 activation could be detected using a phospho-ASK1 antibody in TNFα-treated wt or NF-κB-deficient fibroblasts or in ConA-injected mice (H.K., unpublished data). We therefore examined the involvement of JNK phosphatases, which as members of the MKP subgroup of protein tyrosine phosphatases (PTPs) share the PTP signature motif at their catalytic pocket (Figure 2A). A key feature of this motif is the catalytic cysteine which is highly sensitive to oxidation due to its low pK_a (Salmeen et al., 2003; van Montfort et al., 2003). Indeed, several PTPs are transiently inactivated in cells treated with growth factors through oxidation of their catalytic cysteine (Lee et al., 1998; Meng et al., 2002). Inactivation of PTPs

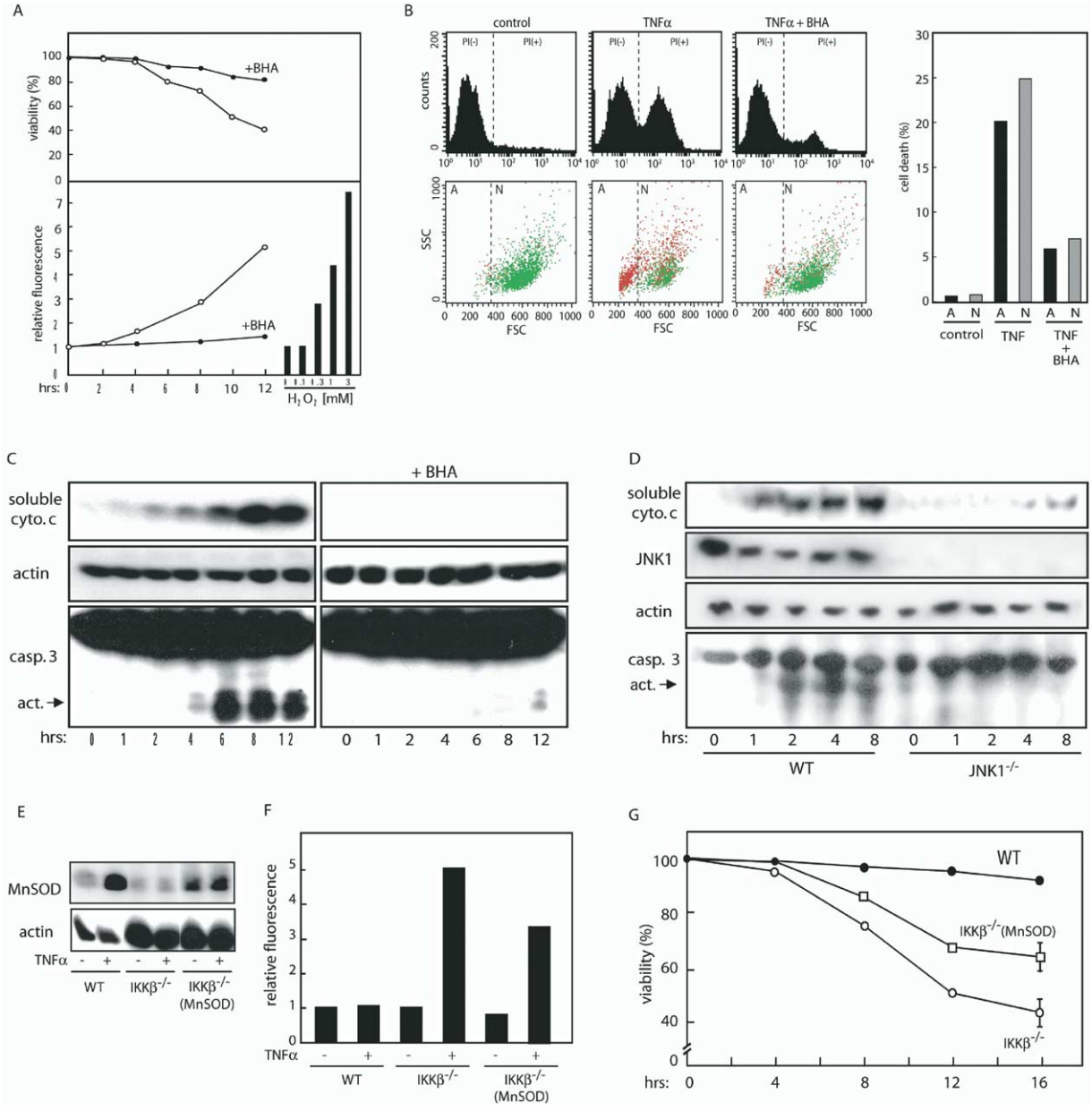

Figure 1. ROS and JNK Are Required for TNFα-Induced Cytochrome c Release, Caspase 3 Cleavage, and PCD

(A) Timecourse of TNFα-induced cell death and H_2O_2 production in *Ikkβ*$^{-/-}$ fibroblasts. Cells were incubated with TNFα in the presence or absence of BHA (100 μM). Cell viability was assessed by Trypan-blue dye exclusion. H_2O_2 production was measured by flow cytometry of cells loaded with 1 μM CM-H_2DCFDA for 30 min prior to each time point. Bar graph: fluorescent intensity of cells loaded with CM-H_2DCFDA and incubated with H_2O_2 for 30 min.

(B) TNFα induces apoptosis and necrosis. *Ikkβ*$^{-/-}$ fibroblasts were left untreated or treated with TNFα without or with BHA. After 12 hr, cell viability and volume were measured by flow cytometry. Upper panels: membrane integrity assessed by dye exclusion using PI. Lower panels: the volume of PI-positive (red dots) and PI-negative (green dots) cells was monitored by side scatter (SSC) versus forward scatter (FSC). Apoptosis (A) is associated with decreased FSC of PI-positive cells. Necrosis (N) correlates with little or no change in FSC of PI-positive cells. Side panel: the percentage of apoptosis (A) and necrosis (N) in the different treatment groups.

(C) BHA suppresses TNFα-induced cytochrome c release and caspase 3 cleavage. *Ikkβ*$^{-/-}$ fibroblasts were incubated with TNFα in the absence or presence of BHA for the indicated periods and cytochrome c release and caspase 3 cleavage (act.) were monitored.

(D) JNK1 is required for cytochrome c release and caspase 3 cleavage in vivo. wt and *Jnk1*$^{-/-}$ mice were injected with 25 mg/kg of ConA. At the indicated times, mice were sacrificed and their livers removed and homogenized. Postmitochondrial supernatants were analyzed for cytochrome c content, caspase 3 cleavage, JNK1, and actin levels.

(E) TNFα induces MnSOD expression in an IKKβ-dependent manner. wt, *Ikkβ*$^{-/-}$, and *Ikkβ*$^{-/-}$ (MnSOD) fibroblasts were incubated with or without TNFα for 8 hr and MnSOD levels were analyzed by immunoblotting.

(F) MnSOD suppresses ROS accumulation. Fibroblasts were incubated without or with TNFα for 8 hr and DCF fluorescence analyzed as in (A).

(G) Timecourse of TNFα-induced cell death in wt, *Ikkβ*$^{-/-}$, and *Ikkβ*$^{-/-}$ (MnSOD) fibroblasts.

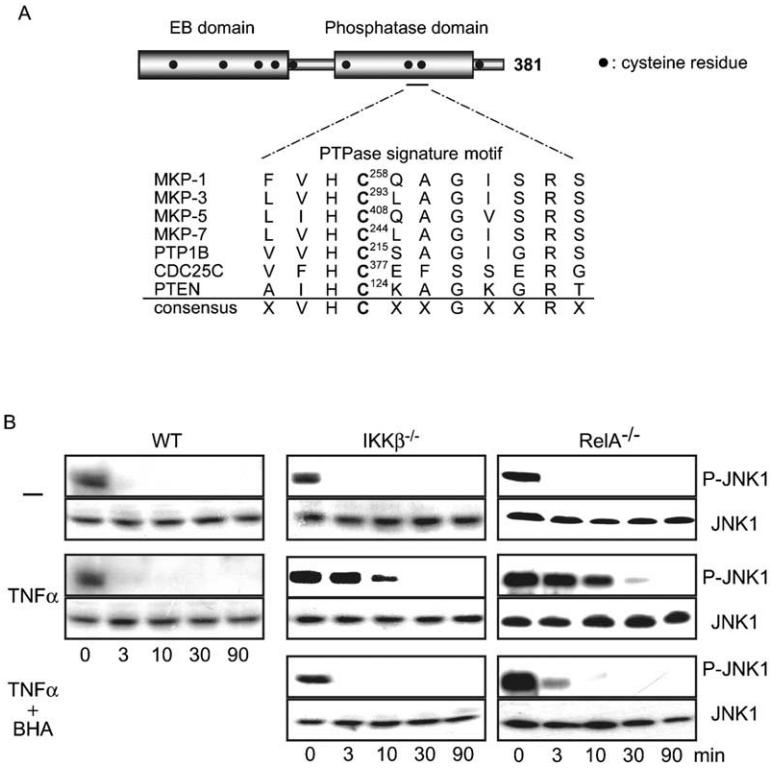

Figure 2. TNFα Inhibits JNK Phosphatase Activity in NF-κB-Deficient Fibroblasts

(A) Schematic representation of MKP-3 structural organization and the conserved catalytic motif.

(B) TNFα down-modulates JNK-phosphatase activity. Cells were incubated without or with TNFα in the absence or presence of BHA for 8 hr, and lysed. Lysates were incubated with phosphorylated JNK1 at 37°C for the indicated periods and JNK1 dephosphorylation was monitored by immunoblotting with anti-phospho-JNK antibody.

is thought to facilitate and prolong activation of their target kinases.

To investigate whether JNK phosphatases are inactivated during TNFα treatment, we incubated activated JNK1 with lysates of untreated and TNFα-treated cells in a phosphatase buffer and monitored dephosphorylation of its activation loop with an anti-phospho-JNK antibody. Rapid and invariant JNK1 dephosphorylation was seen upon incubation with lysates of nonstimulated wt or NF-κB-deficient cells (Figure 2B). Treatment of wt fibroblasts with TNFα had no effect on JNK phosphatase activity, but diminished JNK dephosphorylation was found upon incubation with lysates of TNFα-treated NF-κB-deficient cells (Figure 2B). Coincubation of these cells with BHA prevented the TNFα-induced decrease in JNK phosphatase activity. Hence, sustained JNK activation is likely to entail inactivation of JNK phosphatases.

TNFα-Induced MKP Oxidation

To examine TNFα-induced MKP inhibition in more detail, we focused on MKP-1, MKP-3, MKP-5, and MKP-7, all of which function as JNK phosphatases (Masuda et al., 2001; Sanchez-Perez et al., 2000; Tanoue et al., 2001). Initially, HeLa cells were treated with various concentrations of H_2O_2, and lysates were prepared and separated by SDS-PAGE in the absence of β-mercaptoethanol (βME) or other reducing agents. As oxidized MKP-1 is rapidly degraded by the proteasome (data not shown), we incubated cells with a proteasome inhibitor, MG132, to inhibit its degradation. Immunoblotting revealed a marked dose-dependent shift in the electrophoretic mobility of MKP-1 in H_2O_2-treated cells to high molecular weight (HMW) species that barely entered the gel (Figure 3A). Incubation of the lysates with βME abolished this mobility shift, suggesting that the slow migrating MKP-1 forms are mixed disulfides between MKP-1 and HMW proteins (Figure 3A). Next, HeLa cells were transfected with expression plasmids encoding Flag-tagged wt MKPs or mutant counterparts in which the catalytic cysteine was replaced with a serine. Again, immunoblot analysis revealed a marked dose-dependent shift in the electrophoretic mobility of all MKPs in H_2O_2-treated cells (Figures 3B and 3C and data not shown). Formation of these HMW forms, which barely entered the gel, was suppressed by conversion of the catalytic cysteine to a serine. Note that instead of full-length MKP-7, which is poorly expressed, we used a deletion mutant which retained the catalytic domain. Even this truncated protein formed HMW complexes upon oxidation.

Next, we examined the effect of endogenously produced ROS generated by incubation of *Ikkβ*$^{-/-}$ fibroblasts with TNFα. wt and *Ikkβ*$^{-/-}$ fibroblasts were transfected with either wt or mutant Flag-tagged MKP-1 and MKP-3 and Myc-tagged MKP-5 expression vectors. Immunoblot analysis demonstrated that TNFα treatment of transfected *Ikkβ*$^{-/-}$ cells induced HMW forms of wt MKP-1, MKP-3, and MKP-5 that were abolished by incubation with βME (Figures 3D, 3F, and 3G). Appearance of the oxidized MKP forms, which was not seen in wt cells, was prevented by incubating *Ikkβ*$^{-/-}$ cells with BHA, suggesting that endogenously generated ROS cause MKP oxidation. As seen with H_2O_2, MKP oxidation was prevented by replacement of the catalytic cysteine with serine (Figures 3D and 3F). Ti-

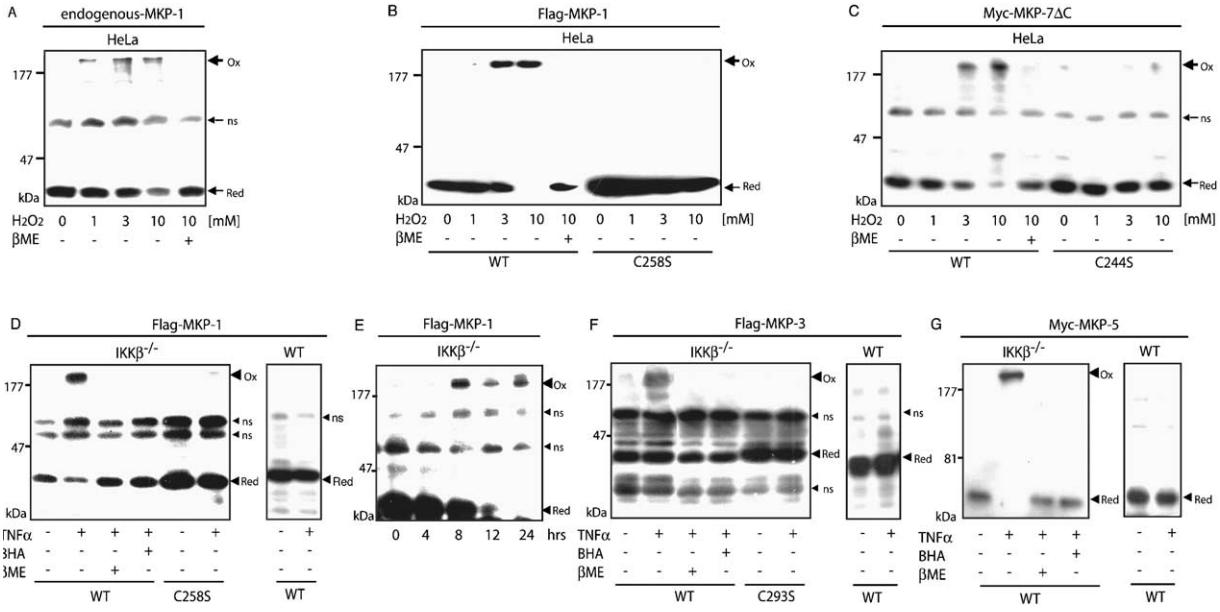

Figure 3. MKPs Are Oxidized in TNFα-Treated IKKβ-Deficient Cells

(A) HeLa cells were treated with the indicated concentrations of H_2O_2 for 10 min in the presence of MG132 (50 μM).

(B–G) Flag-tagged MKP-1 (B, D, and E), Myc-tagged MKP-7ΔC (C), Flag-tagged MKP-3 (F), Myc-tagged MKP-5 (G), and their catalytic cysteine mutants were transiently expressed in HeLa cells, wt, or *Ikkβ*$^{-/-}$ fibroblasts, as indicated. HeLa cells were treated with H_2O_2 for 10 min (B and C). wt and *Ikkβ*$^{-/-}$ fibroblasts were treated with TNFα in the absence or presence of BHA for 12 hr (D, F, and G) or the indicated times (E). Cells expressing MKP-1 were also incubated with MG132 to block degradation of oxidized MKP-1. All cells were lysed in a buffer containing 10 mM NEM to prevent oxidation of cysteines during sample preparation. Lysates were fractionated by SDS-PAGE in the absence or presence of 250 mM βME as indicated and analyzed by immunoblotting. MKP oxidation was monitored by changes in electrophoretic mobility. Ox—oxidized MKP, Red—reduced MKP, ns—nonspecific band.

mecourse analysis revealed that the shift in MKP-1 electrophoretic mobility was barely detectable at 4 hr of incubation of *Ikkβ*$^{-/-}$ cells with TNFα but was nearly maximal at 8 hr (Figure 3E).

Consistent with these biochemical data, immunofluorescent staining of transfected Cos7 cells revealed aggregation of Flag-MKP-3 after H_2O_2 treatment (Figure 4A). Such aggregates were not formed by Flag-MKP-3(C293S). Similar results were obtained when wt and mutant Flag-MKP-3 were expressed in *Ikkβ*$^{-/-}$ fibroblasts. In this case, treatment with TNFα induced the aggregation of wt Flag-MKP-3 but did not alter the distribution of a Flag-MKP-3 (C293S) mutant (Figure 4B).

To confirm the critical role of the catalytic cysteine in MKP oxidation, we generated and analyzed nine different mutants of MKP-3, replacing each cysteine with a serine. Only the catalytic cysteine mutant, C293S, did not exhibit any phosphatase activity and was resistant to H_2O_2-induced oxidation (Figure S4). Similar results were obtained either in vitro or in intact cells, indicating that the catalytic cysteine is responsible for MKP oxidation.

MKP Oxidation Results in Formation of Sulfenic Acid

Cysteine oxidation by H_2O_2 results in formation of either sulfenic (-SOH), sulfinic (-SO_2H), or sulfonic (-SO_3H) acid, representing addition of one, two, or three oxygens, respectively. Whereas sulfenic acid is relatively unstable and readily reacts with other thiols to generate a disulfide, which can be reverted to the original cysteine upon reduction, the sulfonic and sulfinic acid forms represent irreversible end products (Claiborne et al., 1999). To determine which form of oxidation was inflicted upon the catalytic cysteine of MKP-3 we incubated purified GST-MKP-3 with H_2O_2. This resulted in dose-dependent inhibition of phosphatase activity with an IC_{50} around 0.3 mM H_2O_2 (Figure 5A). Fully oxidized MKP-3 was partially reactivated by addition of DTT, indicating that reversible and irreversible modifications were involved (Figure 5A). To measure the redox state of its catalytic cysteine, GST-MKP-3 was incubated with the thiol reactive fluorescent dye fluorescein-5-maleimide (F5M). Unoxidized MKP-3 was efficiently labeled by F5M, whereas MKP-3 pretreated with 3 mM H_2O_2 was hardly labeled at all (Figure 5A). Addition of DTT to oxidized MKP-3 partially recovered its F5M reactivity and phosphatase activity. The H_2O_2-induced electrophoretic mobility shifts were also dose dependent and paralleled inhibition of phosphatase activity and F5M reactivity (Figure 5B). Nonetheless, no obvious mobility shift was detected upon incubation of MKP-3 with 0.3 mM H_2O_2, a dose that caused more than 50% inhibition. Although prolonged incubation of purified GST-MPK-3 with H_2O_2 led to formation of large oligomers (Figure 5B), short incubation generated smaller oligomers (Figure S4D).

We used mass spectrometry (MS) to determine the exact oxidation state of C293 or MKP-3. To prevent potential signals caused by oxidation of C287 and M309,

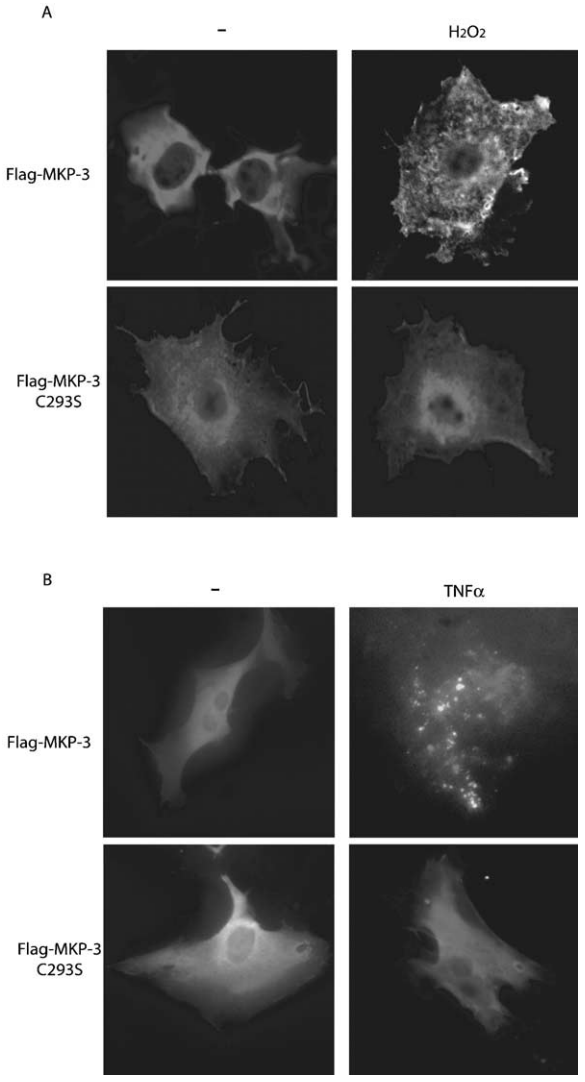

Figure 4. Oxidation-Induced MKP Aggregation in Cells Depends on the Catalytic Cysteine

(A) Cos7 cells and (B) *Ikkβ*$^{-/-}$ fibroblasts were transfected with Flag-tagged wt MKP-3 or its catalytic cysteine mutant (C293S). (A) Cos7 cells were left untreated or treated with 3 mM H_2O_2 for 10 min. (B) *Ikkβ*$^{-/-}$ fibroblasts were left untreated or treated with TNFα for 12 hr. The cells were fixed, stained with anti-Flag antibody, and analyzed by indirect immunofluorescence.

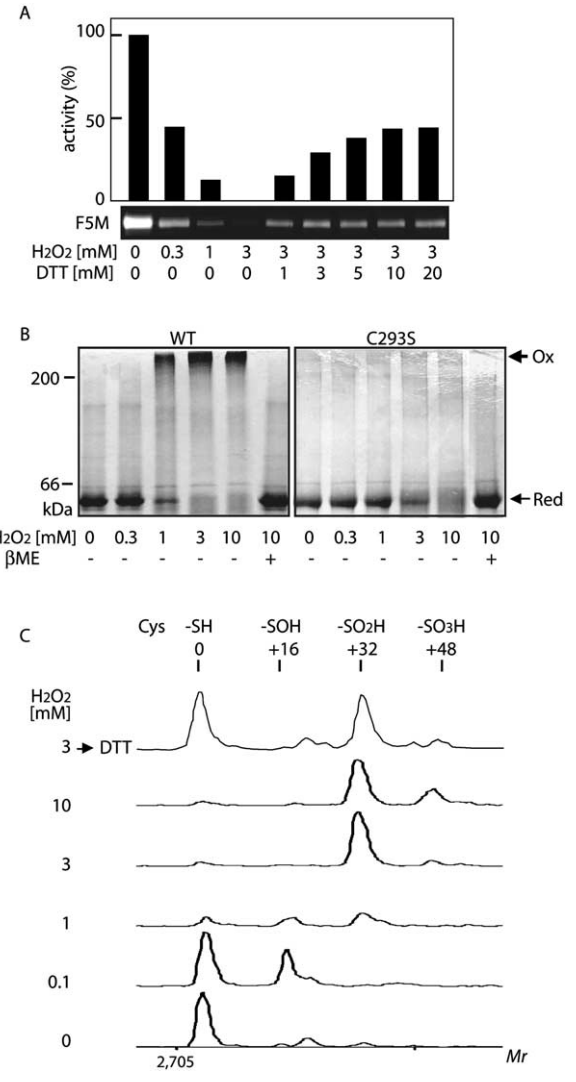

Figure 5. Sulfenic Acid Formation Is Responsible for ROS-Mediated MKP Inactivation

(A) H_2O_2 induces reversible and irreversible MKP-3 inactivation. Purified GST-MKP-3 was treated with 5 mM DTT to reduce its cysteines and then transferred into a DTT-free buffer containing H_2O_2, as indicated. After 10 min, GST-MKP-3 was isolated and transferred into a buffer containing the indicated concentrations of DTT and its activity measured by PNPP hydrolysis (upper panel). After the phosphatase assay, GST-MKP-3 was labeled with the thiol reactive dye F5M, digested with thrombin, and subjected to SDS-PAGE to separate the GST and MKP-3 moieties. The extent of F5M labeling was examined by fluorography (bottom panel).

(B) H_2O_2 induces formation of large GST-MKP-3 complexes. GST-MKP-3 and GST-MKP-3(C293S) were incubated with the indicated concentrations of H_2O_2 for 10 min. The proteins were separated by SDS-PAGE in the absence or presence of 250 mM βME and stained with Coomassie Brilliant Blue (CBB).

(C) H_2O_2 induces sulfenic acid formation. Purified MKP-3(C287S/M309S) was treated with the indicated concentrations of H_2O_2 followed by digestation with lysil-endopeptidase. The digests were subjected to MS in the absence or presence of 100 mM DTT. The shift in molecular mass (Mr) of the active site-containing peptide was analyzed.

which are located within the same proteolytic fragment as C293, we converted these residues to serines. The redox sensitivity of MKP-3 and its activity were not changed by these mutations (data not shown). Purified MKP-3(C287S/M309S) was treated with H_2O_2 and digested with lysil-endopeptidase. The mass of the peptide containing C293 was monitored by MS. Incubation with H_2O_2 decreased the signal corresponding to reduced C293 and shifted the relative molecular mass by +16, +32, or +48 dalton (corresponding to sulfenic, sulfinic, or sulfonic acid derivatives, respectively) (Figure 5C). The +32 and +48 shifts were not fully abolished by DTT addition but the signal corresponding to fully reduced C293 had reappeared (Figure 5C). This is con-

sistent with the results in Figure 5A. As the +16 shift corresponding to the sulfenic acid was not detected in fully oxidized MKP-3 before or after DTT treatment, the reduced cysteine must have originated from a disulfide. Thus, H_2O_2 can cause either irreversible C293 oxidation to sulfinic or sulfonic acid or reversible oxidation to a sulfenic acid or a disulfide. Although conversion of C293 to sulfenic acid inhibits MKP-3 activity, it does not retard its electrophoretic mobility. The latter requires formation of disulfides.

Inhibition of MKP Activity Allows TNFα to Kill wt Cells

Cellular reductases are essential for maintaining the activity of many enzymes, especially those that rely on a reduced cysteine (Georgiou and Masip, 2003). We examined whether oxidized MKP-3 can be reduced in cells. HeLa cells expressing Flag-MKP-3 were incubated with 3 mM H_2O_2 for 15 min and then switched to normal medium. Within 10 min of H_2O_2 removal, reduced MKP-3 had reappeared (Figure 6A). Cellular reductases depend on either reduced glutathione (GSH) or Trx as reducing equivalents (Georgiou and Masip, 2003; Holmgren, 2000). To evaluate the relative importance of the two for reduction of oxidized MKP-3, we incubated transfected HeLa cells with either buthioninesulfoximine (BSO), an inhibitor of GSH synthesis, or 2,4-dinitro-1-chlorobenzene (DNCB), which prevents recycling of Trx by inhibiting TrxR. Whereas BSO had little effect (although it decreased the level of GSH at least 90%), DNCB completely prevented reduction of MKP-3 (Figure 6A). Similar results were obtained with Flag-MKP-1, Myc-MKP-5, and Myc-MKP-7 (data not shown). Therefore, reduction of oxidized MKPs requires Trx-dependent reductases, such as peroxiredoxins (Georgiou and Masip, 2003).

Incubation of wt fibroblasts with DNCB or H_2O_2 prolonged JNK activation and potentiated the response to TNFα (Figure 6B), which in untreated cells is transient (Figure S1A). Importantly, treatment of wt fibroblasts with DNCB, H_2O_2, or As^{3+}, a potent inhibitor of JNK phosphatases (Cavigelli et al., 1996), allowed their killing by TNFα (Figure 6C). This enhancement of TNFα-induced PCD was not seen in *Jnk1*$^{-/-}$ fibroblasts (Figure 6C). Thus, the effect of the different inhibitors on cell killing is relatively specific and depends on JNK activation.

To genetically test the involvement of MKP inactivation in TNFα-mediated PCD, we transfected wt fibroblasts with expression vectors encoding either wt or catalytically inactive MKPs, which act in a dominant-negative fashion (Masuda et al., 2001; Sanchez-Perez et al., 2000). Whereas wt MKPs suppressed TNFα-mediated transient JNK activation, the MKP mutants enhanced and prolonged JNK activity (Figure 6D). Next, we transfected wt fibroblasts with a GFP expression vector along with either wt or catalytically inactive MKP expression vectors and monitored the viability of transfected cells. TNFα did not diminish viability of cells transfected with either GFP plasmid alone or together with wt MKP expression vectors, but in cells cotransfected with mutant MKP expression vectors TNFα markedly decreased cell viability (Figure 6E). These results strongly suggest that MKP inactivation plays an important role in JNK-dependent TNFα-induced PCD.

The Antioxidant BHA Prevents ConA-Induced Liver Injury

Intravenous administration of ConA to mice causes severe liver injury that depends on TNFα and JNK signaling and is potentiated by inhibition of NF-κB (Maeda et al., 2003). To examine whether TNFα-induced ROS are involved in sustained JNK activation during ConA-induced liver failure, we examined the levels of reduced GSH in livers of untreated and treated mice because the DCFDA fluorescence assay cannot be used in vivo. Injection of wt mice with the subtoxic dose of 10 mg/kg ConA modestly decreased the level of GSH, but injection of wt mice with the toxic dose of 25 mg/kg ConA or injection of *Ikkβ*$^{\Delta hep}$ mice with 10 mg/kg ConA, to which they respond with fulminant hepatitis (Maeda et al., 2003), resulted in a marked drop in GSH (Figure 7A). A more modest decrease in reduced GSH was seen in *Jnk1*$^{-/-}$ mice, suggesting a possible contribution of JNK to oxidative stress (Figure 7A). Thus, as in tissue culture, exposure of hepatocytes to a cytotoxic form of TNFα (which is induced by ConA) results in oxidative stress that is exacerbated by absence of IKKβ. Exposure of wt mice to 25 mg/kg of ConA also resulted in decreased JNK phosphatase activity (Figure 7B) and prolonged JNK activation (Figure 7C).

To prevent ROS accumulation, we fed mice with a BHA-containing diet for 2 days before ConA administration. In mice kept on a normal diet, injection of ConA markedly increased the circulating levels of alanine aminotransferase (ALT), a marker of liver necrosis, but this increase was strongly suppressed by BHA administration (Figure 7D). BHA administration also reduced the number of apoptotic, TUNEL-positive hepatocytes induced by ConA (Figure 7E) as well as the magnitude and duration of ConA-induced JNK activation (Figure 7C). Thus, ROS are likely to be important mediators of ConA-induced liver damage, as seen in fibroblasts.

Another TNFα- and JNK-dependent response is liver regeneration (Schwabe et al., 2003; Yamada et al., 1997). By contrast to ConA-induced liver failure, liver regeneration after partial hepatectomy is associated with modest and transient JNK activation (Schwabe et al., 2003). The magnitude and kinetics of JNK activation in response to partial hepatectomy were not affected by BHA administration (Figure 7C), which also had no effect on the kinetics or extent of liver regeneration (Figures 7F and 7G).

Discussion

ROS, MKPs, and Modulation of TNFα Signaling

Binding of TNFα to TNFR1 generates diverse biological outcomes, including the diametrically opposed responses of cell proliferation and cell death (Wajant et al., 2003). The exact outcome depends on the context and cell type in which TNFR1 is activated. Although activation of TNFR1 by soluble TNFα is insufficient for triggering PCD (Grell et al., 1995; Maeda et al., 2003), the death response is strongly augmented by inhibition

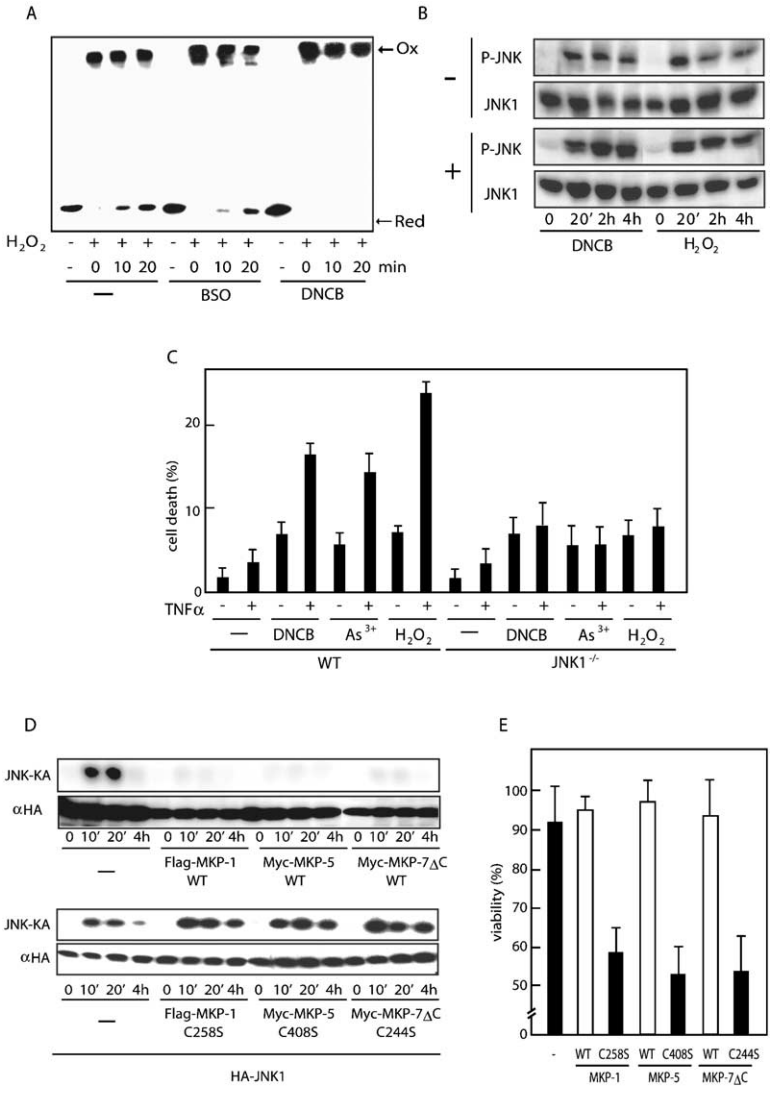

Figure 6. Inactivation of MKPs Stimulates TNFα-Induced PCD through JNK Activation

(A) Reduction of oxidized MKPs depends on the Trx system. Flag-tagged MKP-3 was transiently expressed in HeLa cells. Following incubation with 300 μM BSO for 24 hr or 100 μM DNCB for 15 min, the cells were incubated with 3 mM H_2O_2 and 10 μg/ml cycloheximide for 15 min to oxidize previously synthesized Flag-MKP-3. The medium was changed to H_2O_2-free medium containing cycloheximide. At the indicated times, cells were lysed in a buffer containing 10 mM NEM and MKP-3 oxidation was analyzed by SDS-PAGE as described in Figure 3.

(B) Activation of JNK by DNCB and H_2O_2. wt fibroblasts were incubated for the indicated times without or with TNFα in the absence or presence of DNCB (10 μM) or H_2O_2 (1 mM) as indicated. The cells were lyzed and JNK activation determined by immunoblotting with anti-phospho-JNK antibody.

(C) Diverse inhibitors of MKP activity enhance TNFα-induced PCD. wt or *Jnk1*$^{-/-}$ fibroblasts were incubated without or with TNFα for 4 hr. DNCB (10 μM), As^{3+} (100 μM), or H_2O_2 (1 mM) were added as indicated and the cells were incubated for 4 more hr. Cell viability was assessed by Trypan-blue exclusion. Results are presented as averages ± SD (n = 3).

(D) Catalytically inactive MKPs prolong JNK activation. wt fibroblasts were transfected with an HA-JNK1 plasmid (1 μg) together with expression vectors (4 μg each) for wt or catalytically inactive MKPs. After 24 hr, cells were treated with 50 ng/ml of TNFα, and JNK activity was determined by an immunecomplex kinase assay (KA) after immunoprecipitation with anti-HA (αHA) antibodies.

(E) Catalytically inactive MKPs enable TNFα-induced PCD of wt cells. Fibroblasts were transfected with a GFP plasmid (1 μg) together with expression vectors (4 μg each) for wt or catalytically inactive MKPs. After 24 hr, cells were treated with TNFα for 8 hr and viability of GFP-positive cells was assessed by PI dye exclusion and flow cytometry. Results are presented as averages ± SD (n = 3).

of NF-κB (Karin and Lin, 2002; Varfolomeev and Ashkenazi, 2004) or concomitant activation of TNFR2 (Wajant et al., 2003), both of which potentiate JNK activation (Maeda et al., 2003). Whereas the IKK-NF-κB pathway is an established negative regulator of the death response and its inhibition by cytokines, drugs or toxins may cause various TNFα-mediated pathologies, the role of the JNK cascade in determining the biological response to TNFα has been more elusive. Initial experiments using protein synthesis inhibitors either found no role for JNK in modulation of TNF-induced cell death (Liu et al., 1996) or ascribed it with a protective function (Natoli et al., 1997). However, more recent experiments carried out in cells in which NF-κB activation was genetically inhibited demonstrated that JNK activation promotes TNF-induced cell death (De Smaele et al., 2001; Deng et al., 2003; Tang et al., 2001; Varfolomeev and Ashkenazi, 2004). Nonetheless, JNK activity per se is not a simple on-off switch and its level and duration determine its biological function, as transient and modest JNK activation is required for liver regeneration (Schwabe et al., 2003), whereas prolonged and robust JNK activation promotes cell death (Lin, 2003). Hence, the mechanisms that control the level of JNK activity serve as important contextual modulators of the biological outcome of TNFR1 engagement. Our results show an important role for ROS, whose production is induced by TNFα but is negatively regulated by NF-κB, in enhancing the magnitude and duration of JNK activation through inhibition of JNK phosphatases.

Inhibition or downregulation of NF-κB prolongs JNK activation not only in mammals but also in *Drosophila* cells (Park et al., 2004). Nonetheless, the mechanism underlying this crosstalk had remained elusive. NF-κB was suggested to attenuate JNK activation through induction of *GADD45β* (De Smaele et al., 2001) or *XIAP* (Tang et al., 2001), but neither proposal received support from studies conducted in Gadd45β- (Amanullah

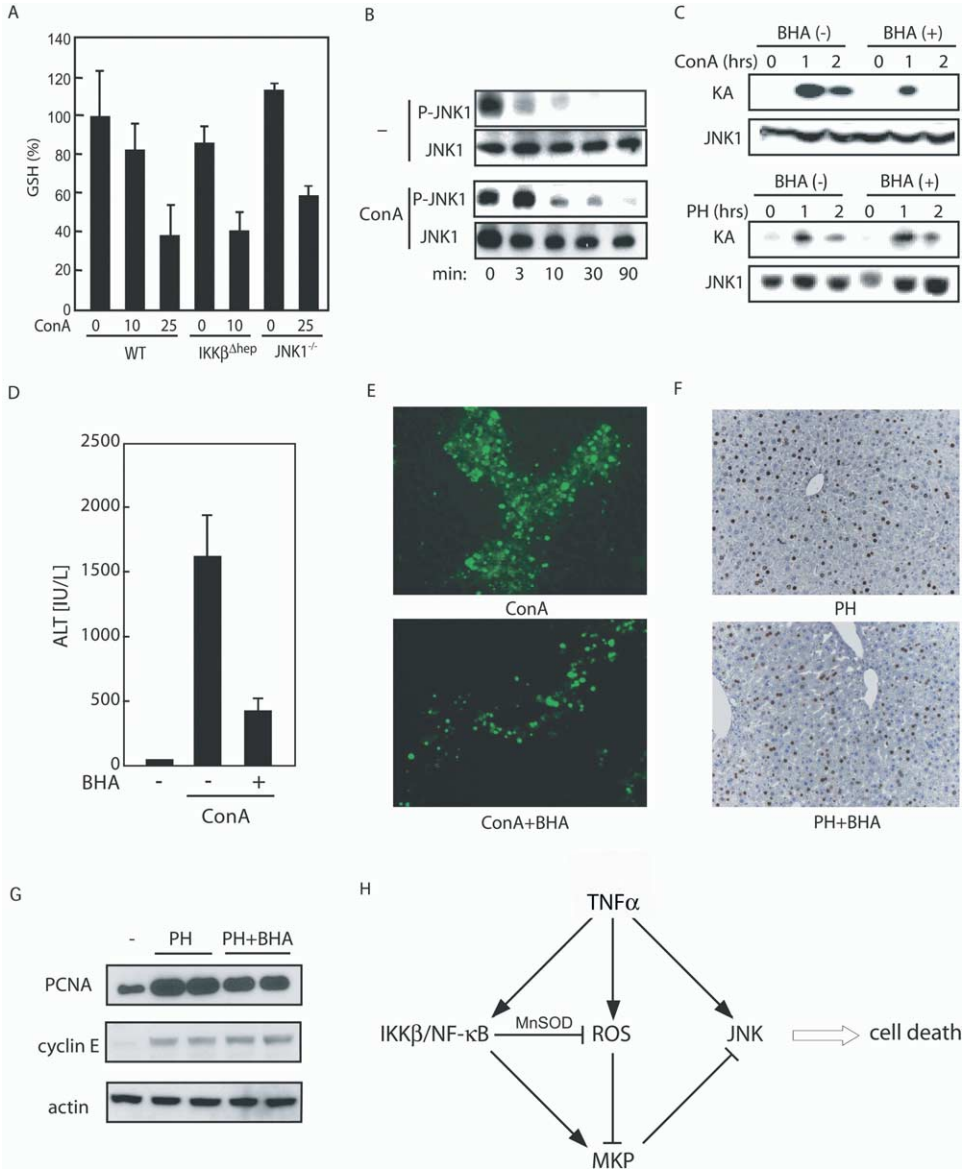

Figure 7. Oxidative Stress Is iInvolved in ConA-Induced Liver Damage but Not in Liver regeneration

(A) wt and *Ikk*$\beta^{\Delta hep}$ mice were injected with the indicated doses of ConA (mg/kg). After 8 hr, mice were sacrificed and their livers removed to determine GSH concentration. The average level of GSH in livers of untreated wt mice was given a value of 100%. Results are averages ± SD.

(B) ConA treatment downmodulates JNK phosphatase activity. Mice (wt) were injected with 25 mg/kg ConA in PBS and sacrificed 8 hr later. Liver cell lysates were prepared and examined for JNK phosphatase activity as described in Figure 2B.

(C) Consumption of BHA-containing diet shortens the duration of JNK activation after ConA administration but not after partial hepatectomy. JNK activity in liver was measured after ConA injection or partial hepatectomy in mice fed either a normal diet or a diet containing 7 g/kg BHA.

(D and E) Consumption of BHA-containing diet prevents ConA-induced liver damage. Mice (wt) were fed either a normal or a BHA-containing diet for 2 days prior to ConA injection. (D) After 8 hr, circulating levels of ALT were analyzed. Results are averages ± SD (n = 3). (E) The extent of liver apoptosis was evaluated by TUNEL staining. Typical fields of stained liver sections are shown.

(F and G) BHA does not interfere with liver regeneration. Mice fed either normal or BHA-containing diet were subjected to partial hepatectomy. (F) To determine the rate of DNA synthesis, mice were injected with BrdU at 34 hr after liver resection and sacrificed 2 hr later. BrdU incorporation into hepatocytes was examined by immunohistochemical analysis. (G) The extent of PCNA and cyclin E expression at 36 hr after partial hepatectomy (each lane represents a different mouse) or in a sham-treated mouse was determined by immunoblotting.

(H) NF-κB modulates the TNFα-induced death response through control of ROS accumulation and MKP activity. TNFα induces NF-κB and JNK activation, as well as ROS production. NF-κB prevents ROS accumulation in part through induction of MnSOD. This preserves MKP activity, some of which is induced by NF-κB, and ensures transient JNK activation and cell survival. If NF-κB is inhibited, ROS accumulate and MKPs are inhibited, leading to sustained JNK activation and cell death.

et al., 2003) or Xiap- (Kucharczak et al., 2003) deficient cells. It was also not clear why GADD45β or XIAP should only affect JNK activation by TNFα and not by IL-1. The observation that TNFα but not IL-1 stimulates ROS production in NF-κB-deficient cells provided strong insight to the NF-κB-JNK crosstalk (Sakon et al., 2003), and a role for ROS in modulating TNFα-induced PCD was also demonstrated (Wong et al., 1989). Although ROS accumulation and prolonged JNK activation were initially connected to TNFα-induced necrosis (Sakon et al., 2003), a more recent study demonstrated their involvement in TNFα-induced apoptosis (Pham et al., 2004). Our results show that ROS production contributes to both forms of death in cultured fibroblasts and in mice. Regardless of the PCD phenotype, none of the previous studies had explained how ROS production prolongs JNK activation, and a defined molecular target whose activity is affected by ROS was not heretofore identified. Our current findings identify JNK phosphatases as critical molecular targets for ROS action in the context of TNFα-induced PCD.

The magnitude and duration of JNK activity are determined by the balance between activating kinases and inhibitory phosphatases. The MAP3K ASK1 was suggested to mediate JNK activation in response to H_2O_2 (Takeda et al., 2003), but neither others (Sakon et al., 2003) nor we could find evidence for its involvement in sustained JNK activation in NF-κB-deficient cells. Instead, we found that in such cells TNFα inhibits the activity of JNK phosphatases, which belong to the MKP group of PTPs. At least four MKPs, MKP-1, -3, -5, and -7, are inhibited through oxidation of their catalytic cysteine in TNFα-treated NF-κB-deficient cells or upon incubation with H_2O_2. It is well established that the catalytic cysteine of PTPs is much more sensitive to oxidation than other cysteines because of its unusually low pK_a (Salmeen et al., 2003; van Montfort et al., 2003), leading to the suggestion that cysteine oxidation is an important mode of their regulation. While most studies demonstrating oxidative PTP inhibition have relied on treatment with exogenous H_2O_2 (Lee et al., 1998; Savitsky and Finkel, 2002), partial and transient PTP oxidation was seen after growth factor stimulation (Lee et al., 1998; Meng et al., 2002). Our results show extensive and long-lasting MKP oxidation in TNFα-treated NF-κB-deficient cells. This activity involves conversion of the catalytic cysteine to sulfenic acid, which can be reversed by incubation with reducing agents or upon removal of oxidant pressure through Trx-dependent reductases.

The same chemical properties of the catalytic cysteine needed for MKP enzymatic activity are also responsible for its sensitivity to H_2O_2, thereby precluding generation of catalytically active and oxidation-resistant MKP mutants that could have been useful for blocking persistent JNK activation. Nonetheless, using catalytically inactive MKP mutants, we show that reduced MKP activity allows TNFα to kill NF-κB-competent cells in a JNK-dependent manner. A similar effect is achieved by inhibition of TrxR, whose activity is required for reactivation of oxidized MKPs.

Interestingly, NF-κB is an important positive regulator of MKP activity. At least one MKP, MKP-3, is encoded by an NF-κB-dependent gene (Li et al., 2002). Another important NF-κB target gene codes for MnSOD, the enzyme responsible for conversion of superoxide radicals (O_2^-) to H_2O_2 and their eventual elimination through peroxidases, which convert H_2O_2 to H_2O (Wong et al., 1989). Another NF-κB target gene encoding ferritin heavy chain (FHC) is also involved in conversion of H_2O_2 to H_2O and is likely to act downstream of MnSOD (Pham et al., 2004). As O_2^- and H_2O_2 are important inhibitors of MKP activity, by inhibiting their accumulation NF-κB maintains MKP activity, thereby preventing prolonged JNK activation (Figure 7H).

The Role of ROS in Programmed Cell Death

While the results discussed above strongly support a role for ROS in PCD, the relationships between the two are complex. Some investigators find ROS to mediate only TNFα-induced necrosis (Sakon et al., 2003), whereas others implicate it in TNFα-induced apoptosis (Pham et al., 2004). We find that TNFα can induce both forms of PCD in cultured cells and in mice once *Ikkβ* has been inactivated, and that both programs are inhibited by BHA. Timecourse analysis reveals that H_2O_2 accumulation parallels cytochrome c release from mitochondria. Importantly, inhibition of ROS accumulation or reduced JNK activity prevent cytochrome c release and caspase 3 cleavage. Although the origin of TNFα-induced ROS remains to be identified, they are likely to originate in the mitochondrion, where inhibition of electron transfer results in O_2^- buildup (Cai and Jones, 1998; Newmeyer and Ferguson-Miller, 2003). This assumption is supported by the ability of the mitochondrial-specific enzyme MnSOD to suppress TNFα-induced ROS accumulation. Although the initial leakage of cytochrome c from the mitochondrion may not be sufficient for disruption of electron transfer and enhancement of ROS production (Newmeyer and Ferguson-Miller, 2003), the latter may augment cytochrome c release through oxidation of cardiolipin (Iverson and Orrenius, 2004; Nomura et al., 2000). Cardiolipin oxidation may enhance mitochondrial targeting of tBID (Lutter et al., 2000), a proapoptotic cleavage product of BID that is generated in response to TNFα-mediated caspase 8 activation (Li et al., 1998; Luo et al., 1998).

While the exact mechanism through which ROS promote cytochrome c release remain to be elucidated, our results strongly suggest that critical targets for H_2O_2-induced oxidation in the TNFα-triggered cell death process are the MKPs. By controlling the duration of JNK activation, whose activity is required for TNFα-induced cytochrome c release and caspase 8 activation, through either jBID formation (Deng et al., 2003) or a cFLIP-dependent mechanism (L.C. and M.K., unpublished data), as well as TNFα-induced necrosis, the MKPs act as a switch that determines the outcome of TNFα signaling. High MKP activity prevents cell death, whereas low MKP activity promotes sustained JNK activation and enhances cell death (Figure 7H).

As discussed above, partial hepatectomy leads to transient JNK activation that is required for liver regeneration (Schwabe et al., 2003), a TNFα-dependent response (Yamada et al., 1997). Feeding mice with BHA has no effect on this response because it does not interfere with transient JNK activation. However, BHA

protects mice from ConA-induced liver failure, a response that requires sustained JNK activation. Given the potential complications and augmented necrotic response associated with caspase inhibitors (Cauwels et al., 2003) and the emerging role of caspase 8 in cell survival (Perfettini and Kroemer, 2003), we propose that mitochondrially targeted antioxidants may present a preferred and viable strategy for therapeutic intervention with fulminant liver failure and even chronic diseases, such as viral hepatitis and alcoholic cirrhosis.

Experimental Procedures

Plasmids, Cells, and Transfection

MKP-1 and MKP-3 cDNAs were amplified by the polymerase chain reaction (PCR) from a human cDNA library. MKP-5, MKP-5(C258S), MKP-7ΔC, and MKP-7ΔC(C244S) expression vectors were provided by Dr. E. Nishida (Kyoto University, Japan). Different substitution mutations were introduced into the MKP-1 and MKP-3 cDNAs by PCR. The MnSOD expression plasmid was provided by Dr. T.Y. Aw (Louisiana State University). Fibroblasts derived from *Ikkβ*$^{-/-}$, *RelA*$^{-/-}$, or *Jnk1*$^{-/-}$ mouse embryos, Cos7, and HeLa cells were cultured in DMEM plus 10% fetal calf serum (FCS). Plasmids were transfected into cells using Lipofectamine and Lipofectamine Plus (Invitrogen) following manufacturer's instructions.

Immunoblot Analysis

Whole-cell lysates were prepared in a buffer containing 20 mM Tris-HCl (pH 7.4), 10 mM EGTA, 10 mM $MgCl_2$, 1 mM benzamidine, 60 mM β-glycerophosphate, 1 mM Na_3VO_4, 20 mM NaF, 1 μM APMSF, 1 μg/ml aprotinin, 10 μg/ml pepstatin, 10 μg/ml leupeptin, 1 mM DTT, and 1% Triton X-100. After 20 min centrifugation at 16,000 × *g* at 4°C, the supernatants were gel separated. For cytosolic extracts, cells were suspended in 50 mM PIPES (pH 7.4), 50 mM KCl, 5 mM EGTA, 2 mM $MgCl_2$, 10 μM cytochalasin, and 1 mM DTT. Following 20 min incubation on ice, 220 mM mannitol and 68 mM glycerol were added, and cells were lysed in a Dounce homogenizer. After 20 min centrifugation at 16,000 × *g* at 4°C the supernatants were gel separated, transferred to nylon membranes, and immunoblotted with antibodies against Flag, Myc, actin (Sigma), phospho-JNK, phospho-p38 (Cell Signaling), JNK1, p38α (Santa Cruz), cytochrome c (Pharmingen), MnSOD (UBI), and caspase 3 (BD Transduction Labs).

Measurement of ROS Production

Fibroblasts (2×10^5 cells) were plated on 35 mm dishes and loaded with CM-H_2DCFDA (Molecular Probes). After 30 min, cells were collected and analyzed using a flow cytometer (FACS Caliber) and the CellQuest computer program.

Kinase and Phosphatase Assays

JNK immunecomplex kinase assay was performed as described (Maeda et al., 2003) using an anti-JNK1 antibody (Santa Cruz) and GST-cJun(1–79) as a substrate. To measure MKP-3 activity, GST-MKP-3 was incubated with 20 mM p-nitrophenyl phosphate (PNPP) in a phosphatase buffer containing 20 mM Tris-HCl (pH 7.4), 1 mM $MnCl_2$, and 0.1 mM $MgCl_2$ at 37°C, and A415 was monitored as a measure of substrate hydrolysis. To measure total JNK phosphatase activity, cells or livers were homogenized in 50 mM Tris-HCl (pH 7.4), 250 mM NaCl, 3 mM EDTA, 3 mM EGTA, 1% Triton X-100, 2 mM DTT, 1 mM APMSF, 1 μg/ml aprotinin, 10 μg/ml pepstatin, and 10 μg/ml leupeptin. After 20 min centrifugation at 16,000 × *g* at 4°C, JNK1/2 were removed from the supernatants by immunoprecipitation, and the immunodepleted lysates were mixed with phosphorylated JNK1 isolated from HeLa cells and incubated at 37°C. The reactions were terminated by addition of 2% SDS and separated by SDS-PAGE. Dephosphorylation of phospho-JNK1 was monitored by immunoblotting.

Mass Spectrometry

Purified MKP-3 was digested with lysil-endopeptidase (Roche). The digests (500 fmol) were combined with a 10-fold excess of matrix solution containing 10 mg/ml α-cyano-4-hydroxycinnamic acid, 50% acetonitrile, and 0.1% trifluoroacetic acid and analyzed by matrix-assisted laser desorption ionization time-of-flight (MALDI-TOF) MS using a Voyager DE-PRO mass spectrometer (Applied Biosystems). Internal reference standards were used for calibration.

Analysis of Protein Oxidation

MKP redox state was monitored by labeling with the thiol-modifying reagent F5M (Molecular probes) or electrophoretic mobility shift on SDS-PAGE under nonreducing conditions. For F5M labeling, GST-MKP-3 was incubated with 0.3 mM F5M in 20 mM Tris-HCl (pH 7.4), 1 mM $MnCl_2$, and 0.1 mM $MgCl_2$ for 5 min on ice. The reaction was stopped with100 mM DTT. After digestion with thrombin for 1 hr at 20°C, the digests were separated by SDS-PAGE. Fluorescence intensities of gel-separated peptides were measured at 490 nm with fluorescence-image analyzer (FLA3000; Fuji Film). For the mobility shift assay, cell lysates were prepared using a buffer containing 20 mM Tris-HCl (pH 7.4), 1% Triton X-100, 10 mM N-ethylmaleimide (NEM), 1 mM APMSF, 1 μg/ml aprotinin, 10 μg/ml pepstatin, and 10 μg/ml leupeptin. The lysates were separated by SDS-PAGE in the presence or absence of βME or DTT and immunoblotted.

Analysis of Liver Injury and Oxidative Stress

Livers were fixed in 4% formaldehyde, dehydrated, embedded in paraffin, and sectioned (5 mm). TUNEL staining was performed as described (Maeda et al., 2003). The serum level of ALT was measured using an assay kit (Sigma). GSH content was measured by an enzymatic assay using glutathione reductase and 5,5′-dithiobis(2-nitrobenzoic acid) (Anderson, 1985).

Supplemental Data

Supplemental Data include four figures and can be found with this article online at http://www.cell.com/cgi/content/full/120/5/649/DC1/.

Acknowledgments

We thank D. Green for helpful discussions, E. Nishida for MKP-5 and MKP-7 vectors, and T.Y. Aw for the MnSOD vector. We also thank M. Mackey and M. Ellisman at the National Imaging Facility at UCSD, supported by NIH, for help with electron microscopy. Research was supported by the Superfund Basic Research Program (NIH 5P42 ES10337) and NIH grants (AI43477, ES04151, and ES06376) to M.K. H.K. was supported by a grant from the 21st Century COE Program and a grant-in-aid from the Ministry of Education, Culture, Sports, Science and Technology of Japan (16570121). S.M. held a postdoctoral fellowship for Research Abroad from the Japan Society for the Promotion of Science. M.K. is an American Cancer Society Research Professor.

Received: August 17, 2004
Revised: November 22, 2004
Accepted: December 22, 2004
Published: March 10, 2005

References

Amanullah, A., Azam, N., Balliet, A., Hollander, C., Hoffman, B., Fornace, A., and Liebermann, D. (2003). Cell signalling: cell survival and a Gadd45-factor deficiency. Nature *424*, 741–742.

Anderson, M.E. (1985). Determination of glutathione and glutathione disulfide in biological samples. Methods Enzymol. *113*, 548–555.

Brenner, D.A., O'Hara, M., Angel, P., Chojkier, M., and Karin, M. (1989). Prolonged activation of jun and collagenase genes by tumor necrosis factor-alpha. Nature *337*, 661–663.

Cai, J., and Jones, D.P. (1998). Superoxide in apoptosis. Mito-

chondrial generation triggered by cytochrome c loss. J. Biol. Chem. *273*, 11401–11404.

Cauwels, A., Janssen, B., Waeytens, A., Cuvelier, C., and Brouckaert, P. (2003). Caspase inhibition causes hyperacute tumor necrosis factor-induced shock via oxidative stress and phospholipase A2. Nat. Immunol. *4*, 387–393.

Cavigelli, M., Li, W., Lin, A., Su, B., Yoshioka, K., and Karin, M. (1996). The tumor promoter arsenite stimulates AP-1 activity by inhibiting a JNK phosphatase. EMBO J. *15*, 6269–6279.

Claiborne, A., Yeh, J.I., Mallett, T.C., Luba, J., Crane, E.J., 3rd, Charrier, V., and Parsonage, D. (1999). Protein-sulfenic acids: diverse roles for an unlikely player in enzyme catalysis and redox regulation. Biochemistry *38*, 15407–15416.

Davis, R.J. (2000). Signal transduction by the JNK group of MAP kinases. Cell *103*, 239–252.

De Smaele, E., Zazzeroni, F., Papa, S., Nguyen, D.U., Jin, R., Jones, J., Cong, R., and Franzoso, G. (2001). Induction of gadd45b by NF-κB downregulates pro-apoptotic JNK signalling. Nature *414*, 308–313.

Deng, Y., Ren, X., Yang, L., Lin, Y., and Wu, X. (2003). A JNK-dependent pathway is required for TNFalpha-induced apoptosis. Cell *115*, 61–70.

Deveraux, Q.L., Takahashi, R., Salvesen, G.S., and Reed, J.C. (1997). X-linked IAP is a direct inhibitor of cell-death proteases. Nature *388*, 300–304.

DiDonato, J.A., Hayakawa, M., Rothwarf, D.M., Zandi, E., and Karin, M. (1997). A cytokine-responsive IκB kinase that activates the transcription factor NF-κB. Nature *388*, 548–554.

Fiers, W., Beyaert, R., Declercq, W., and Vandenabeele, P. (1999). More than one way to die: apoptosis, necrosis and reactive oxygen damage. Oncogene *18*, 7719–7730.

Georgiou, G., and Masip, L. (2003). Biochemistry. An overoxidation journey with a return ticket. Science *300*, 592–594.

Goossens, V., Grooten, J., De Vos, K., and Fiers, W. (1995). Direct evidence for tumor necrosis factor-induced mitochondrial reactive oxygen intermediates and their involvement in cytotoxicity. Proc. Natl. Acad. Sci. USA *92*, 8115–8119.

Grell, M., Douni, E., Wajant, H., Lohden, M., Clauss, M., Maxeiner, B., Georgopoulos, S., Lesslauer, W., Kollias, G., Pfizenmaier, K., et al. (1995). The transmembrane form of tumor necrosis factor is the prime activating ligand of the 80 kDa tumor necrosis factor receptor. Cell *83*, 793–802.

Holmgren, A. (2000). Antioxidant function of thioredoxin and glutaredoxin systems. Antioxid. Redox Signal. *2*, 811–820.

Iverson, S.L., and Orrenius, S. (2004). The cardiolipin-cytochrome c interaction and the mitochondrial regulation of apoptosis. Arch. Biochem. Biophys. *423*, 37–46.

Karin, M., and Lin, A. (2002). NF-κB at the crossroads of life and death. Nat. Immunol. *3*, 221–227.

Kucharczak, J., Simmons, M.J., Fan, Y., and Gelinas, C. (2003). To be, or not to be: NF-κB is the answer–role of Rel/NF-κB in the regulation of apoptosis. Oncogene *22*, 8961–8982.

Lee, S.R., Kwon, K.S., Kim, S.R., and Rhee, S.G. (1998). Reversible inactivation of protein-tyrosine phosphatase 1B in A431 cells stimulated with epidermal growth factor. J. Biol. Chem. *273*, 15366–15372.

Li, H., Zhu, H., Xu, C.J., and Yuan, J. (1998). Cleavage of BID by caspase 8 mediates the mitochondrial damage in the Fas pathway of apoptosis. Cell *94*, 491–501.

Li, X., Massa, P.E., Hanidu, A., Pee, G.W., Aro, P., Savitt, A., Mische, S., Li, J., and Marcu, K.B. (2002). IKKα, IKKβ, and NEMO/IKKγ are each required for the NF-κB-mediated inflammatory response program. J. Biol. Chem. *277*, 45129–45140.

Lin, A. (2003). Activation of the JNK signaling pathway: breaking the brake on apoptosis. Bioessays *25*, 17–24.

Liu, Z.-G., Hu, H., Goeddel, D.V., and Karin, M. (1996). Dissection of TNF receptor 1 effector functions: JNK activation is not linked to apoptosis, while NF-κB activation prevents cell death. Cell *87*, 565–576.

Luo, X., Budihardjo, I., Zou, H., Slaughter, C., and Wang, X. (1998). Bid, a Bcl2 interacting protein, mediates cytochrome c release from mitochondria in response to activation of cell surface death receptors. Cell *94*, 481–490.

Lutter, M., Fang, M., Luo, X., Nishijima, M., Xie, X., and Wang, X. (2000). Cardiolipin provides specificity for targeting of tBid to mitochondria. Nat. Cell Biol. *2*, 754–761.

Maeda, S., Chang, L., Li, Z.-W., Luo, J.-L., Leffert, H.L., and Karin, M. (2003). IKKβ is required for prevention of apoptosis mediated by cell-bound but not by circulating TNFα. Immunity *19*, 725–737.

Masuda, K., Shima, H., Watanabe, M., and Kikuchi, K. (2001). MKP-7, a novel mitogen-activated protein kinase phosphatase, functions as a shuttle protein. J. Biol. Chem. *276*, 39002–39011.

Meng, T.C., Fukada, T., and Tonks, N.K. (2002). Reversible oxidation and inactivation of protein tyrosine phosphatases in vivo. Mol. Cell *9*, 387–399.

Natoli, G., Costanzo, A., Ianni, A., Templeton, D.J., Woodgett, J.R., Balsano, C., and Levrero, M. (1997). Activation of SAPK/JNK by TNFR1 through a noncytotoxic TRAF2-dependent pathway. Science *275*, 200–203.

Newmeyer, D.D., and Ferguson-Miller, S. (2003). Mitochondria: releasing power for life and unleashing the machineries of death. Cell *112*, 481–490.

Nomura, K., Imai, H., Koumura, T., Kobayashi, T., and Nakagawa, Y. (2000). Mitochondrial phospholipid hydroperoxide glutathione peroxidase inhibits the release of cytochrome c from mitochondria by suppressing the peroxidation of cardiolipin in hypoglycaemia-induced apoptosis. Biochem. J. *351*, 183–193.

Park, J.M., Brady, H., Ruocco, M.G., Sun, H., Williams, D., Lee, S.J., Kato, T., Richards, N., Chan, K., Mercurio, F., et al. (2004). Targeting of TAK1 by the NF-κB protein Relish regulates the JNK-mediated immune response in *Drosophila*. Genes Dev. *18*, 584–594.

Perfettini, J.L., and Kroemer, G. (2003). Caspase activation is not death. Nat. Immunol. *4*, 308–310.

Pham, C.G., Bubici, C., Zazzeroni, F., Papa, S., Jones, J., Alvarez, K., Jayawardena, S., De Smaele, E., Cong, R., Beaumont, C., et al. (2004). Ferritin heavy chain upregulation by NF-κB inhibits TNFα-induced apoptosis by suppressing reactive oxygen species. Cell *119*, 529–542.

Sakon, S., Xue, X., Takekawa, M., Sasazuki, T., Okazaki, T., Kojima, Y., Piao, J.H., Yagita, H., Okumura, K., Doi, T., and Nakano, H. (2003). NF-κB inhibits TNF-induced accumulation of ROS that mediate prolonged MAPK activation and necrotic cell death. EMBO J. *22*, 3898–3909.

Salmeen, A., Andersen, J.N., Myers, M.P., Meng, T.C., Hinks, J.A., Tonks, N.K., and Barford, D. (2003). Redox regulation of protein tyrosine phosphatase 1B involves a sulphenyl-amide intermediate. Nature *423*, 769–773.

Sanchez-Perez, I., Martinez-Gomariz, M., Williams, D., Keyse, S.M., and Perona, R. (2000). CL100/MKP-1 modulates JNK activation and apoptosis in response to cisplatin. Oncogene *19*, 5142–5152.

Savitsky, P.A., and Finkel, T. (2002). Redox regulation of Cdc25C. J. Biol. Chem. *277*, 20535–20540.

Schwabe, R.F., Bradham, C.A., Uehara, T., Hatano, E., Bennett, B.L., Schoonhoven, R., and Brenner, D.A. (2003). c-Jun-N-terminal kinase drives cyclin D1 expression and proliferation during liver regeneration. Hepatology *37*, 824–832.

Smith, M.L., Kontny, H.U., Zhan, Q., Sreenath, A., O'Connor, P.M., and Fornace, A.J., Jr. (1996). Antisense GADD45 expression results in decreased DNA repair and sensitizes cells to u.v.-irradiation or cisplatin. Oncogene *13*, 2255–2263.

Takeda, K., Matsuzawa, A., Nishitoh, H., and Ichijo, H. (2003). Roles of MAPKKK ASK1 in stress-induced cell death. Cell Struct. Funct. *28*, 23–29.

Tang, G., Minemoto, Y., Dibling, B., Purcell, N.H., Li, Z.-W., Karin, M., and Lin, A. (2001). Inhibition of JNK activation through NF-κB target genes. Nature *414*, 313–317.

Tanoue, T., Yamamoto, T., Maeda, R., and Nishida, E. (2001). A

Novel MAPK phosphatase MKP-7 acts preferentially on JNK/SAPK and p38 alpha and beta MAPKs. J. Biol. Chem. *276*, 26629–26639.

van Montfort, R.L., Congreve, M., Tisi, D., Carr, R., and Jhoti, H. (2003). Oxidation state of the active-site cysteine in protein tyrosine phosphatase 1B. Nature *423*, 773–777.

Vanden Berghe, T., van Loo, G., Saelens, X., Van Gurp, M., Brouckaert, G., Kalai, M., Declercq, W., and Vandenabeele, P. (2004). Differential signaling to apoptotic and necrotic cell death by Fas-associated death domain protein FADD. J. Biol. Chem. *279*, 7925–7933.

Varfolomeev, E.E., and Ashkenazi, A. (2004). Tumor necrosis factor; an apoptosis JuNKie? Cell *116*, 491–497.

Vercammen, D., Beyaert, R., Denecker, G., Goossens, V., Van Loo, G., Declercq, W., Grooten, J., Fiers, W., and Vandenabeele, P. (1998). Inhibition of caspases increases the sensitivity of L929 cells to necrosis mediated by tumor necrosis factor. J. Exp. Med. *187*, 1477–1485.

Wajant, H., Pfizenmaier, K., and Scheurich, P. (2003). Tumor necrosis factor signaling. Cell Death Differ. *10*, 45–65.

Wong, G.H.W., Elwell, J.H., Oberley, L.W., and Goeddel, D.V. (1989). Manganous superoxide dismutase is essential for cellular resistance to cytotoxicity of tumor necrosis factor. Cell *58*, 923–931.

Yamada, Y., Kirillova, I., Peschon, J.J., and Fausto, N. (1997). Initiation of liver growth by tumor necrosis factor: deficient liver regeneration in mice lacking type I tumor necrosis factor receptor. Proc. Natl. Acad. Sci. USA *94*, 1441–1446.